GNSS and InSAR integration for 3-D crustal deformation in California and western Nevada

Zheng-Kang Shen (UCLA) & Zhen Liu (JPL/Caltech)

SCEC CGM Workshop
Palm Springs, CA
September 7, 2024

GNSS Data

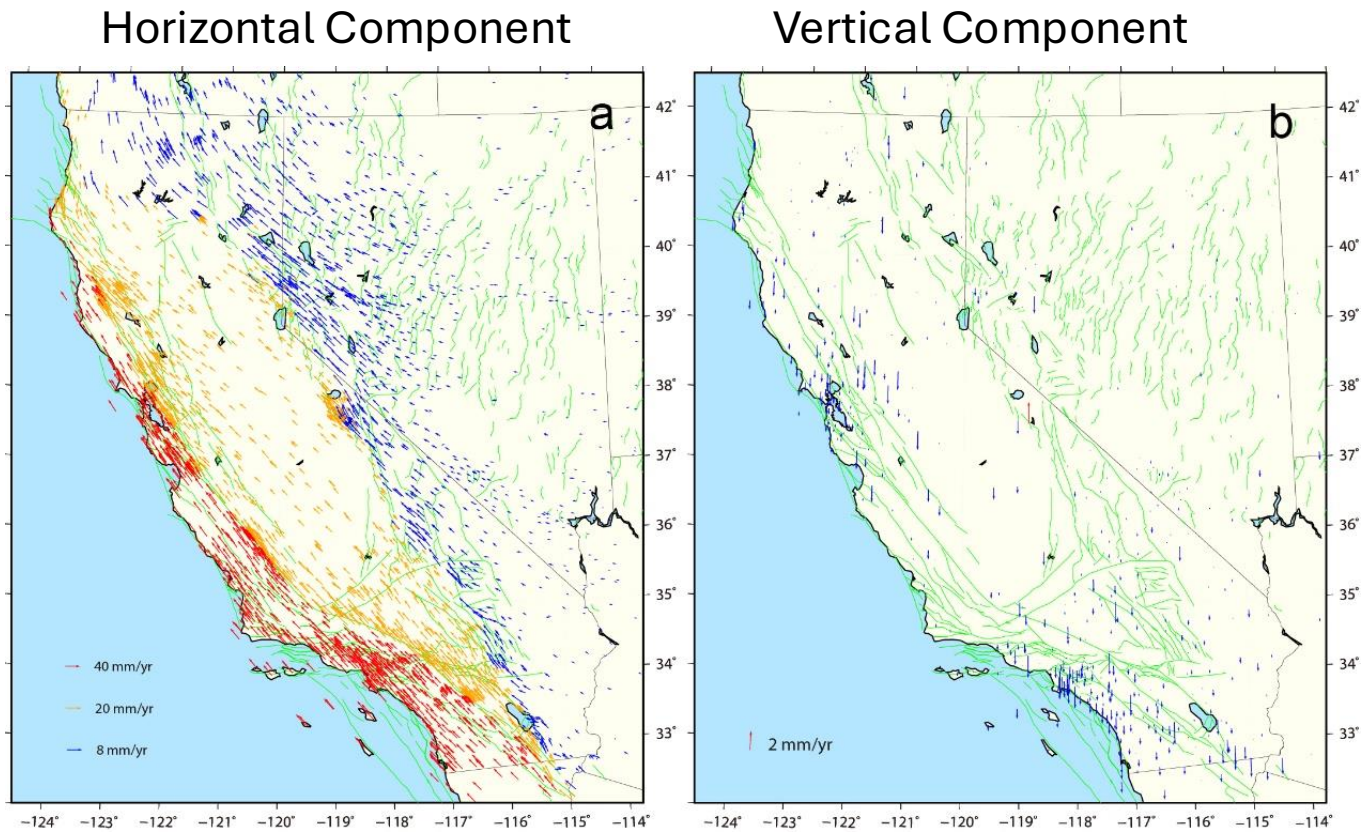

Sources

- 3-D continuous velocity solutions from NASA MEaSUREs project (ftp://sopac-ftp.ucsd.edu/pub/timeseries/measures).
- 2-D horizontal velocity solution from a composite collection of campaign surveys (Zeng, GRL, 2022)
- All solutions - resolved to the North America reference frame

InSAR Data

- ERS/Envisat: 1990s-2010
- Sentinel-1: 2014-2021*
- ALOS-2: 2014-2021

* Tracks subject to Ridgecrest postseismic deformation up to 2019/07/04

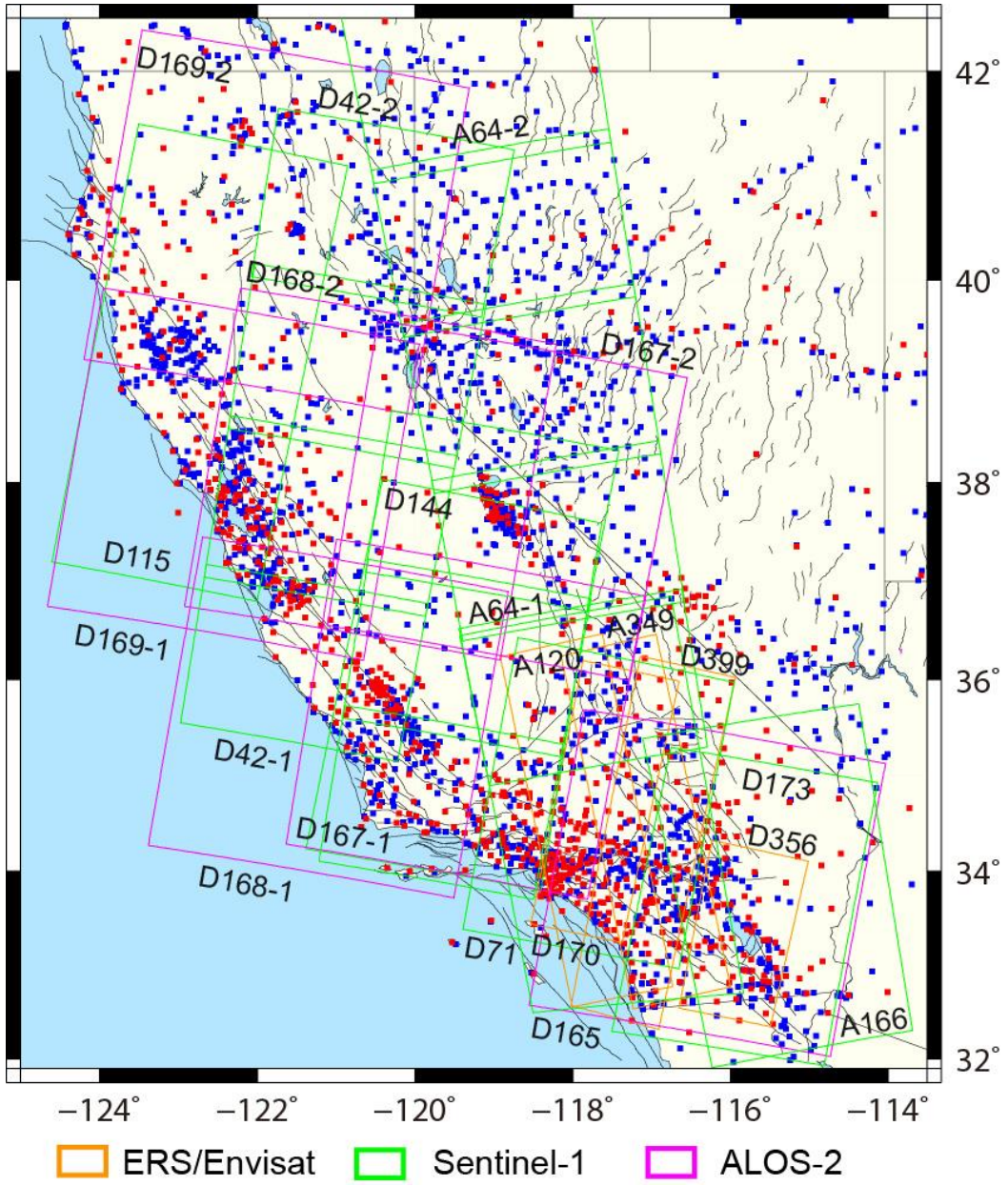

InSAR Data Processing and Uncertainty Estimation

- ERS-1,2 and Envisat: ROI-PAC; Sentinel-1 and ALOS-2: ISCE-2.
- ERS-2 data after 2001 – resolve Doppler ambiguity due to gyroscope failure; Envisat - correct temporally correlated range ramp error caused by long-term local oscillator frequency drift. When applicable, orbital ramp error is corrected through baseline re-estimation.
- Sentinel-1 data - stack processing and adopt enhanced spectral diversity technique to estimate azimuth misregistration between all SLC images in a stack sense [Heresh et al., 2017].
- L-band ALOS-2 –a range split-spectrum approach to estimate and correct ionosphere phase artifacts [[Liang and Fielding, 2017a; Liang et al., 2018].
- A variant of the Small Baseline Subset InSAR time series approach for InSAR time series analysis that incorporate topography dependent troposphere delay and turbulent troposphere noise correction, residual DEM error and earthquake offset estimate [e.g., Liu et al., 2014, 2019].
- Jackknife variance estimation approach to estimate uncertainties of InSAR deformation map [Efron and Stein, 1981]. The RMS of LOS rate difference between GNSS and InSAR is used to scale the InSAR uncertainties during the combination.

InSAR LOS Rate Results

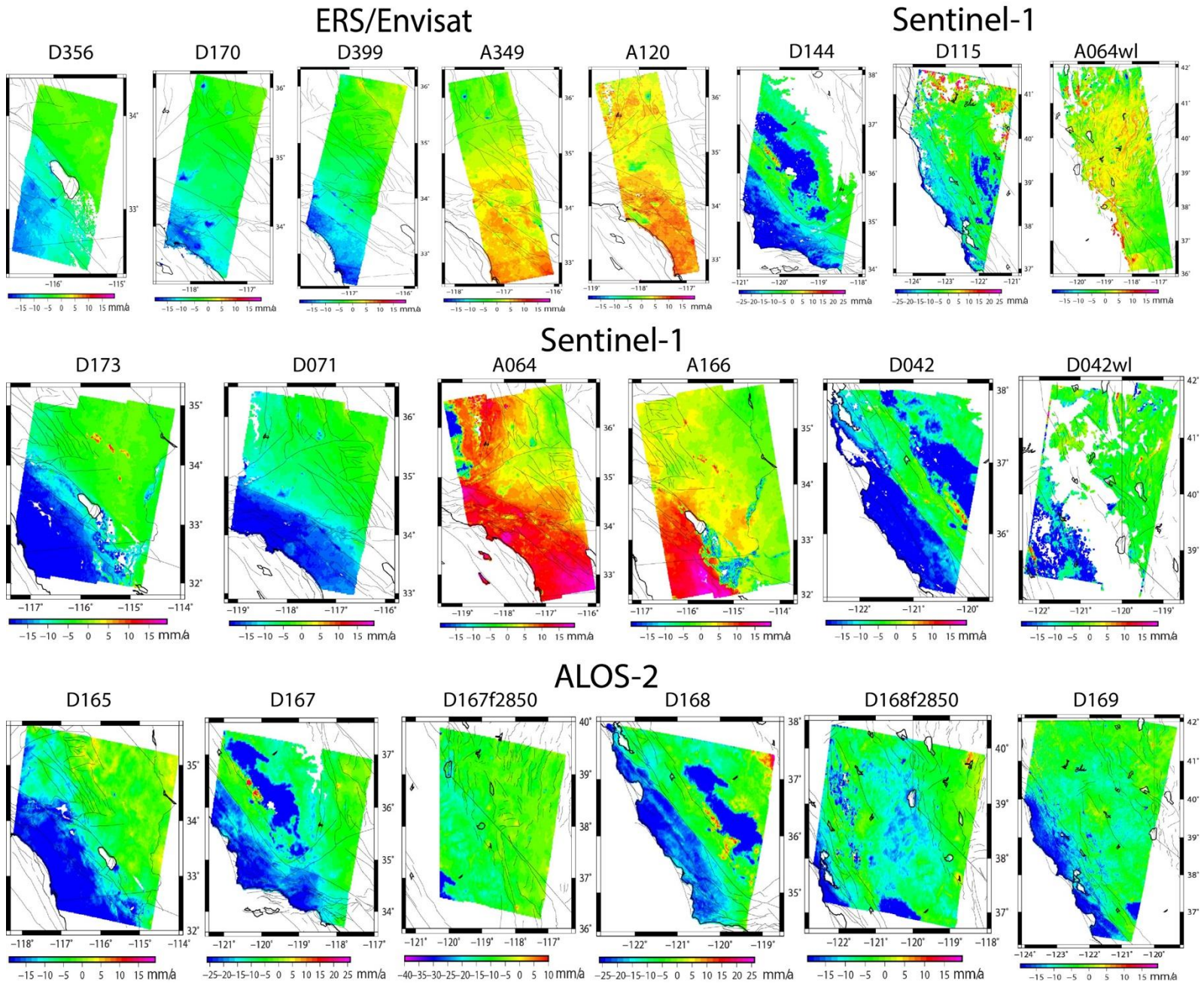

GNSS and InSAR Data Integration Procedure

- Develop an optimal approach to interpolate discrete GNSS velocity data points into a continuous velocity field [Shen et al., 2015; Shen and Liu, 2020]
- Adopt a realistic approach to evaluate uncertainties for InSAR and GNSS measurements and the interpolated GNSS velocities, to be used as weights in the combination
- Resolve the ramp parameters of multiple tracks of InSAR data through global optimization to minimize systematic biases in the solution
- Take an average of InSAR LOS data within small grids and integrate the deramped InSAR and interpolated GNSS data in the grids to solve for 3-D deformation through least-squares regression. The GNSS vertical data are not used in this step.

GPS velocity interpolation

Distance weighting:

$W_i = \exp(-r_i/D)$
D is the distance variable, determined by in situ data strength

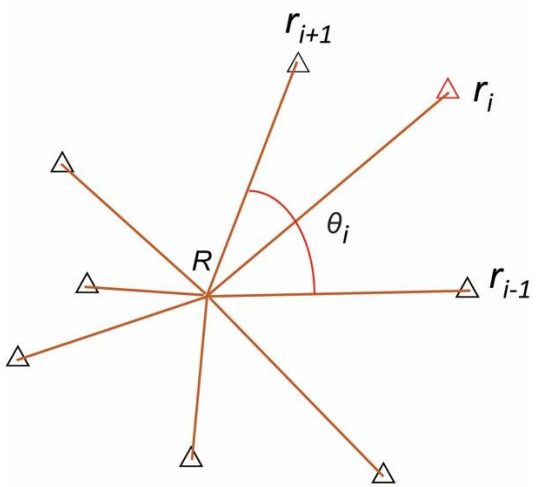

Spatial weighting:

S_i = area of Voronoi cell of i-th site

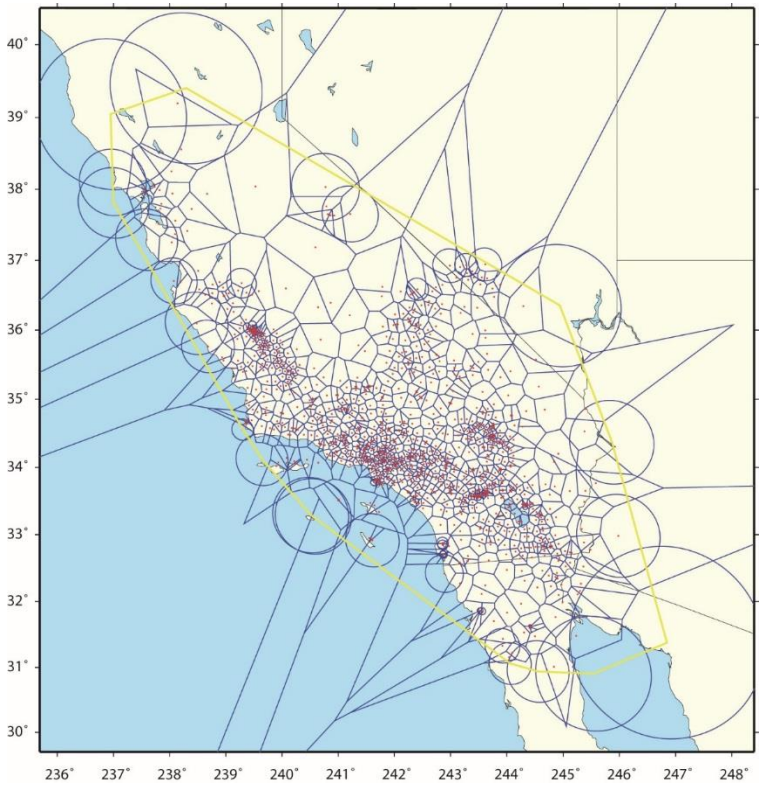

Modeling discontinuity:

Sites located behind a creep fault are excluded from participating interpolation

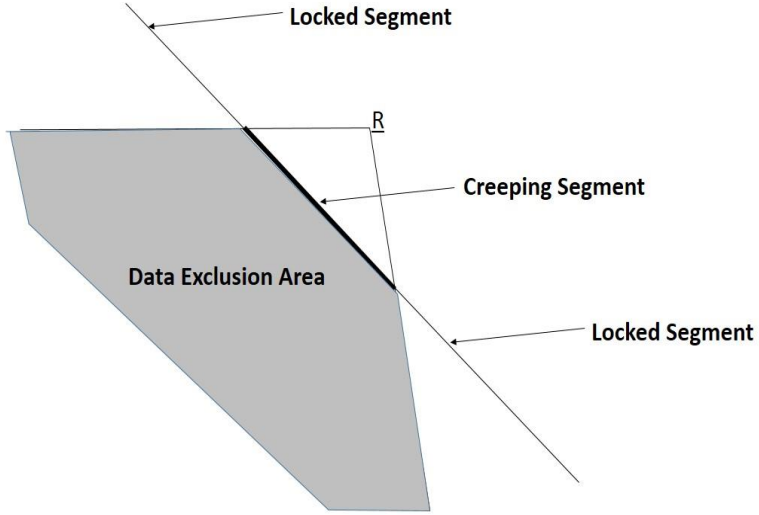

Interpolation Method (Shen et al., 2015)

The displacement data are then linked to the deformation parameters by a linear relationship:

$$\underline{d} = A\,\underline{m} + \underline{\varepsilon} \qquad \underline{\varepsilon} \sim \mathrm{N}(0,C) \qquad (1)$$

where $\underline{d}$ is the data vector, $\underline{m} = (U_x\ U_y\ \omega\ \tau_{xx}\ \tau_{xy}\ \tau_{yy})^{\mathrm{T}}$, U_x and U_y are the translation components, ω is the rotation, and τ_{xx}, τ_{xy}, and τ_{yy} are the horizontal strain components respectively. Equation (1) can also be written as:

$$\begin{bmatrix} Vx_1 \\ Vy_1 \\ Vx_2 \\ Vy_2 \\ \dots \\ Vx_n \\ Vy_n \end{bmatrix} = \begin{bmatrix} 1 & 0 & \Delta y_1 & \Delta x_1 & \Delta y_1 & 0 \\ 0 & 1 & -\Delta x_1 & 0 & \Delta x_1 & \Delta y_1 \\ 1 & 0 & \Delta y_2 & \Delta x_2 & \Delta y_2 & 0 \\ 0 & 1 & -\Delta x_2 & 0 & \Delta x_2 & \Delta y_2 \\ \dots & \dots & \dots & \dots & \dots & \dots \\ 1 & 0 & \Delta y_n & \Delta x_n & \Delta y_n & 0 \\ 0 & 1 & -\Delta x_n & 0 & \Delta x_n & \Delta y_n \end{bmatrix} \begin{bmatrix} U_x \\ U_y \\ \omega \\ \tau_x \\ \tau_{xy} \\ \tau_y \end{bmatrix} + \begin{bmatrix} \varepsilon_{x1} \\ \varepsilon_{y1} \\ \varepsilon_{x2} \\ \varepsilon_{y2} \\ \dots \\ \varepsilon_{xn} \\ \varepsilon_{yn} \end{bmatrix} \qquad (2)$$

where Vx_i and Vy_i are the displacement components of the i-th site at location $\underline{r_i}$. Δx_i and Δy_i are the vector components of $\underline{\Delta R_i} = \underline{r_i} - \underline{R}$.

A least squares solution can be obtained in the form of

$$\underline{m} = (A^T E^{-1} A)^{-1} A^T E^{-1} \underline{d} \qquad (3)$$

where E is a reconstructed variance/covariance matrix, $E \sim E(C, W, S)$.

GNSS and InSAR Data Integration Procedure

- Develop an optimal approach to interpolate discrete GNSS velocity data points into a continuous velocity field [Shen and Liu, 2020]
- Adopt a realistic approach to evaluate uncertainties for GNSS measurements and the interpolated GNSS velocities, to be used as weights in the combination
- Resolve the ramp parameters of multiple tracks of InSAR data through global optimization to minimize systematic biases in the solution
- Take an average of InSAR LOS data within small grids and integrate the deramped InSAR and interpolated GNSS data in the grids to solve for 3-D deformation through least-squares regression. The GNSS vertical data are not used in this step.

Uncertainty estimation for interpolated GNSS velocities

- **Cut-off velocity uncertainties for the horizontal and vertical components**: Using differential velocities of closely located station pairs to estimate the minimum (cut-off) velocity uncertainties: ~0.4 mm/yr for the horiz. and ~0.6 mm/yr for the vert.
- **Uncertainty estimation of interpolated GNSS velocity field**: Using bootstrapping algorithm to estimate the interpolated GNSS velocity uncertainties in an iterative way. Each time an a priori smoothing distance *D* is assumed and used uniformly to evaluate the interpolation velocity uncertainties (σ_a) at all the GNSS sites. In each interpolation the estimation is also performed at each GNSS site without using data of the site, and a difference (δ_d) is calculated at the site between the estimated and original site velocities. Two median uncertainty estimates among all the sites (σ_{am} and δ_{dm}) are compared with, and another iteration is run with a new a priori smoothing distance *D*, until the two median uncertainties are about equal.

Interpolated GNSS velocity field

Horizontal component / uncertainty

Vertical component / uncertainty

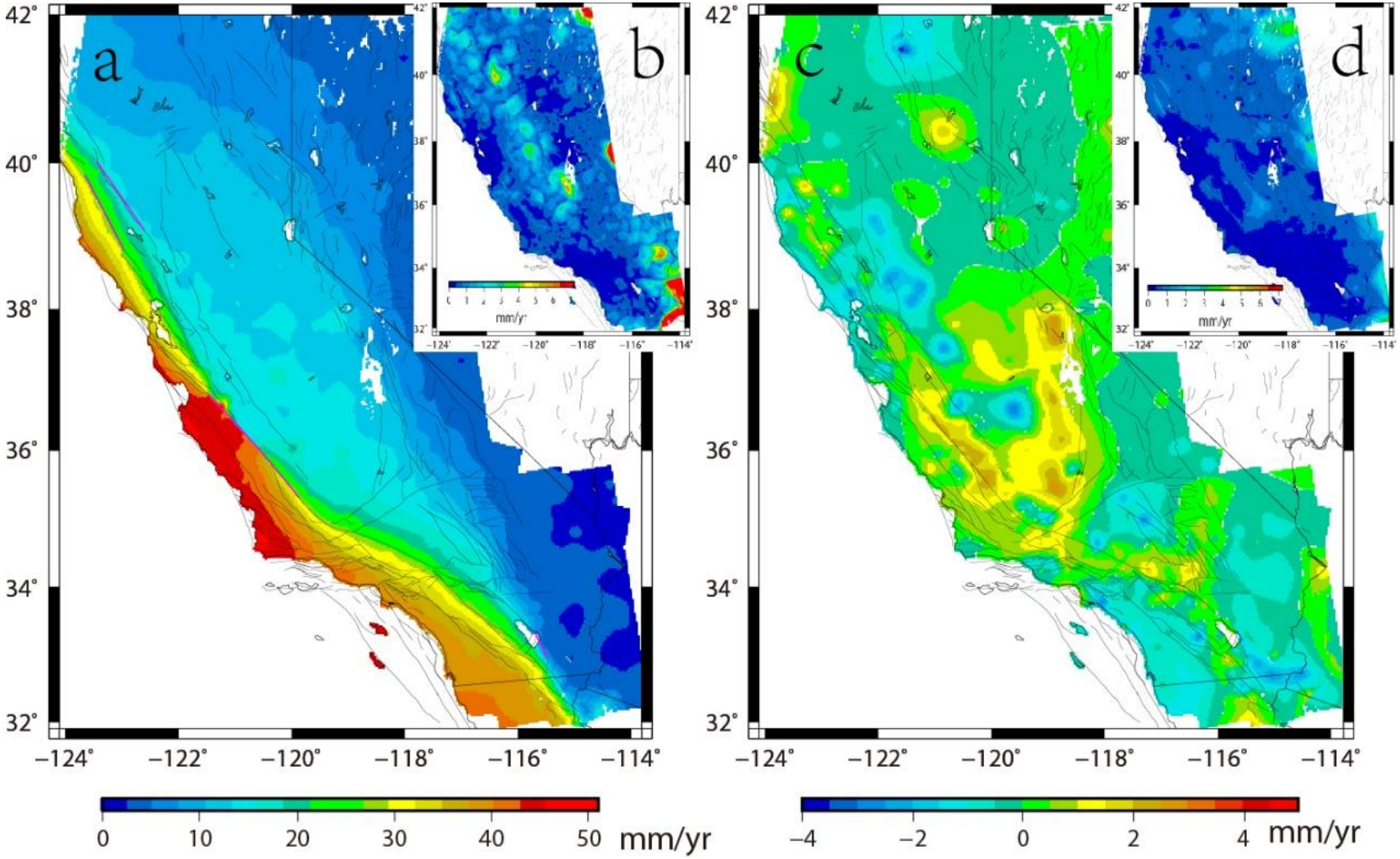

GNSS and InSAR Data Integration Procedure

- Develop an optimal approach to interpolate discrete GNSS velocity data points into a continuous velocity field [Shen and Liu, 2020]
- Adopt a realistic approach to evaluate uncertainties for InSAR and GNSS measurements and the interpolated GNSS velocities, to be used as weights in the combination
- Resolve the ramp parameters of multiple tracks of InSAR data through global optimization to minimize systematic biases in the solution
- Take an average of InSAR LOS data within small grids and integrate the deramped InSAR and interpolated GNSS data in the grids to solve for 3-D deformation through least-squares regression. The GNSS vertical data are not used in this step.

Correction of Offsets and Ramps for InSAR LOS Velocity Data

- Estimate offsets and ramps for InSAR LOS velocities of different tracks which may result from residual orbital error and/or atmospheric noise and not fully corrected for during InSAR data processing.
- The estimation is performed together with the 3-D ground velocities, and some GPS data and their interpolated values are used to stabilize the inversion.
- A global solution for all the parameters involved is solved through a least-squares regression for an optimal estimate of the offsets/ramps.
- Two subsets of GPS data are used in the solution: 1) all the grid points containing GPS velocity observations; 2) interpolated velocities at spatially decimated grid points with multiple InSAR measurements.
- Remove offsets/ramps from the InSAR LOS data and solve for the 3-D velocity at each grid cell through L-S regression with interpolated GNSS velocities and all the LOS data in the cell. Use the adaptive and rescaled GPS and InSAR data uncertainties to weight the data input. Do not include the GPS vertical data in the final solution, due to their relatively large uncertainties and inadequacy to represent fine spatial variation of vertical signals [Shen and Liu, 2020].

GNSS and InSAR Data Integration Procedure

- Develop an optimal approach to interpolate discrete GNSS velocity data points into a continuous velocity field [Shen and Liu, 2020]
- Adopt a realistic approach to evaluate uncertainties for InSAR and GNSS measurements and the interpolated GNSS velocities, to be used as weights in the combination
- Resolve the ramp parameters of multiple tracks of InSAR data through global optimization to minimize systematic biases in the solution
- Take an average of InSAR LOS data within small grids, and integrate the deramped InSAR and interpolated GNSS data in the grids to solve for 3-D deformation through least-squares regression. The GNSS vertical data are not used in this step.

3-D Velocity Solution

Horizontal Component

Ve uncertainty

Vertical Component

Vu uncertainty

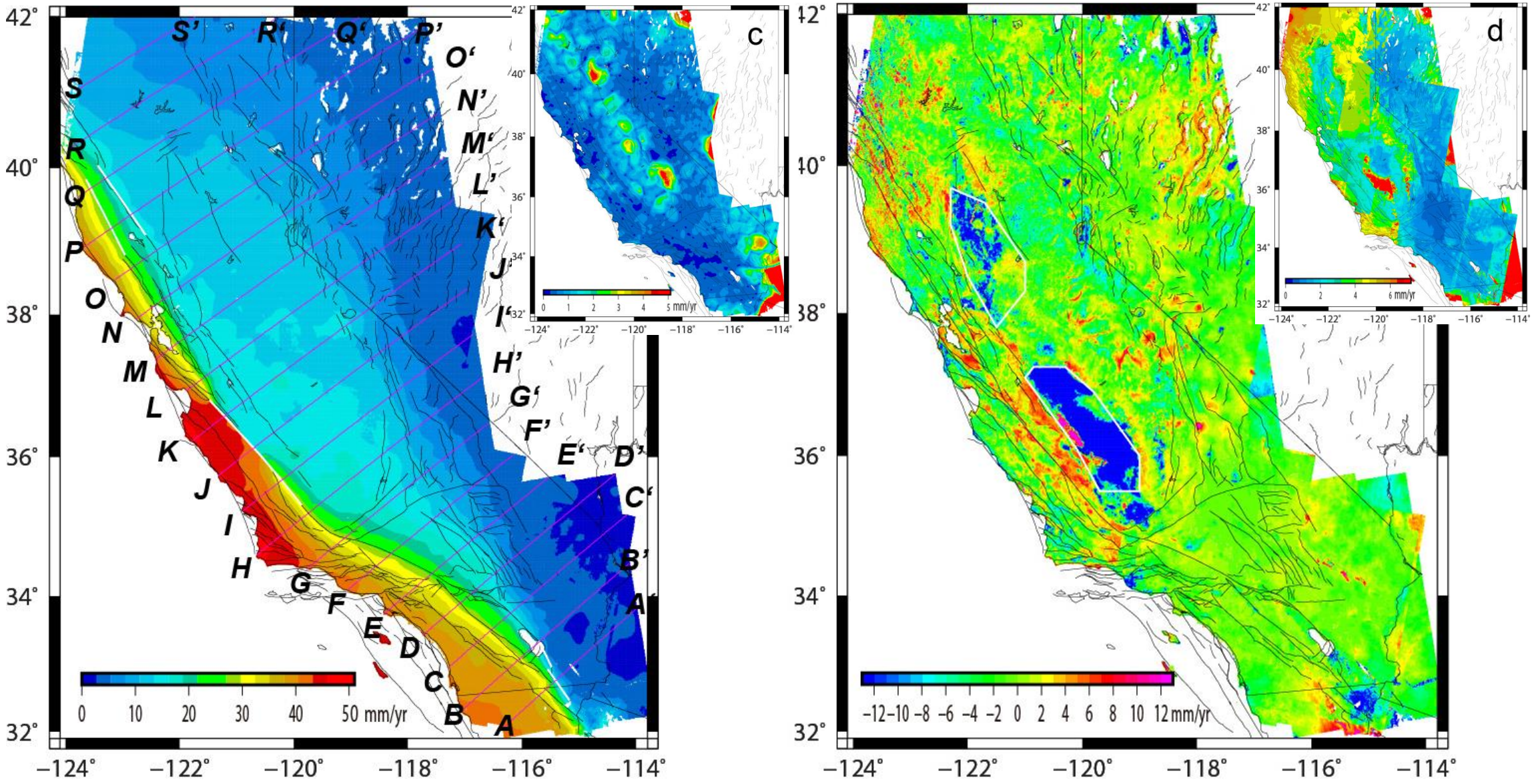

Along Profile Velocity Components wrt Relative Plate Motion Direction

Parallel to RPM

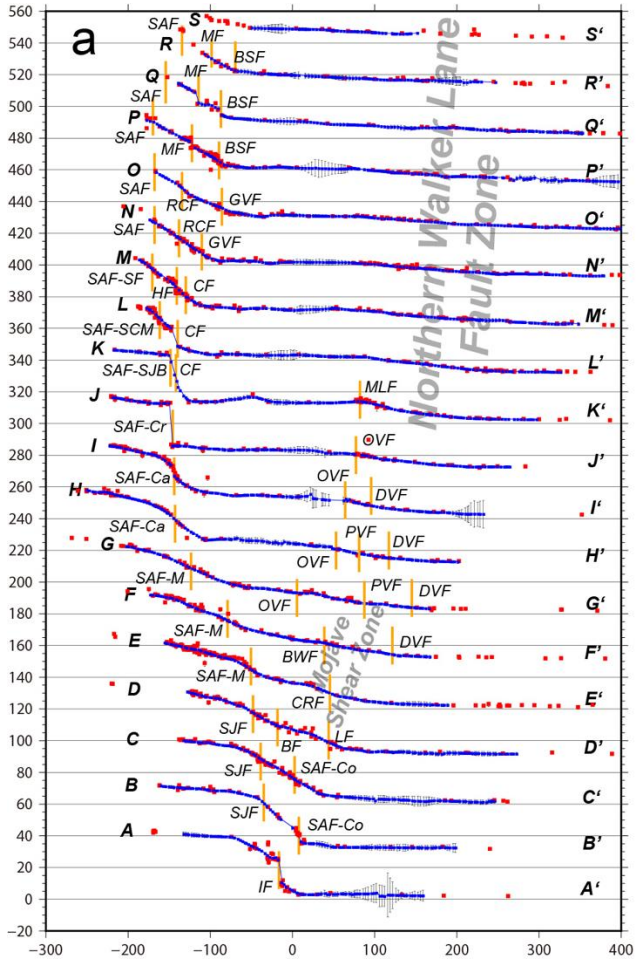

Normal to RPM

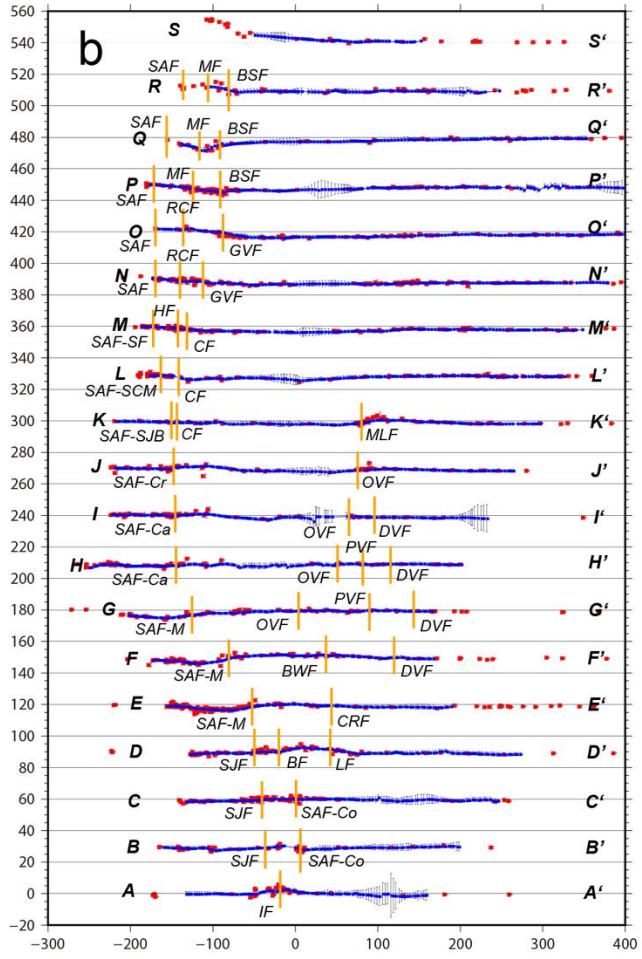

Vertical

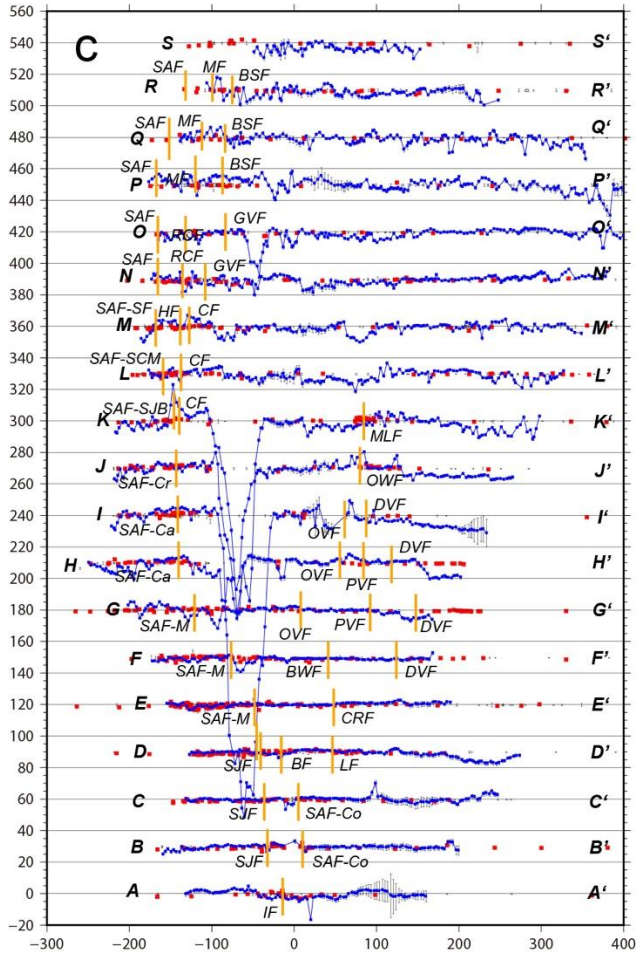

Horizontal deformation is broadly distributed except in central valley and southeastern California, with sinistral motions of ~30-40 mm/yr across the San Andreas and ~10-15 mm/yr across the Walker Lane fault systems.

Regional vertical velocities

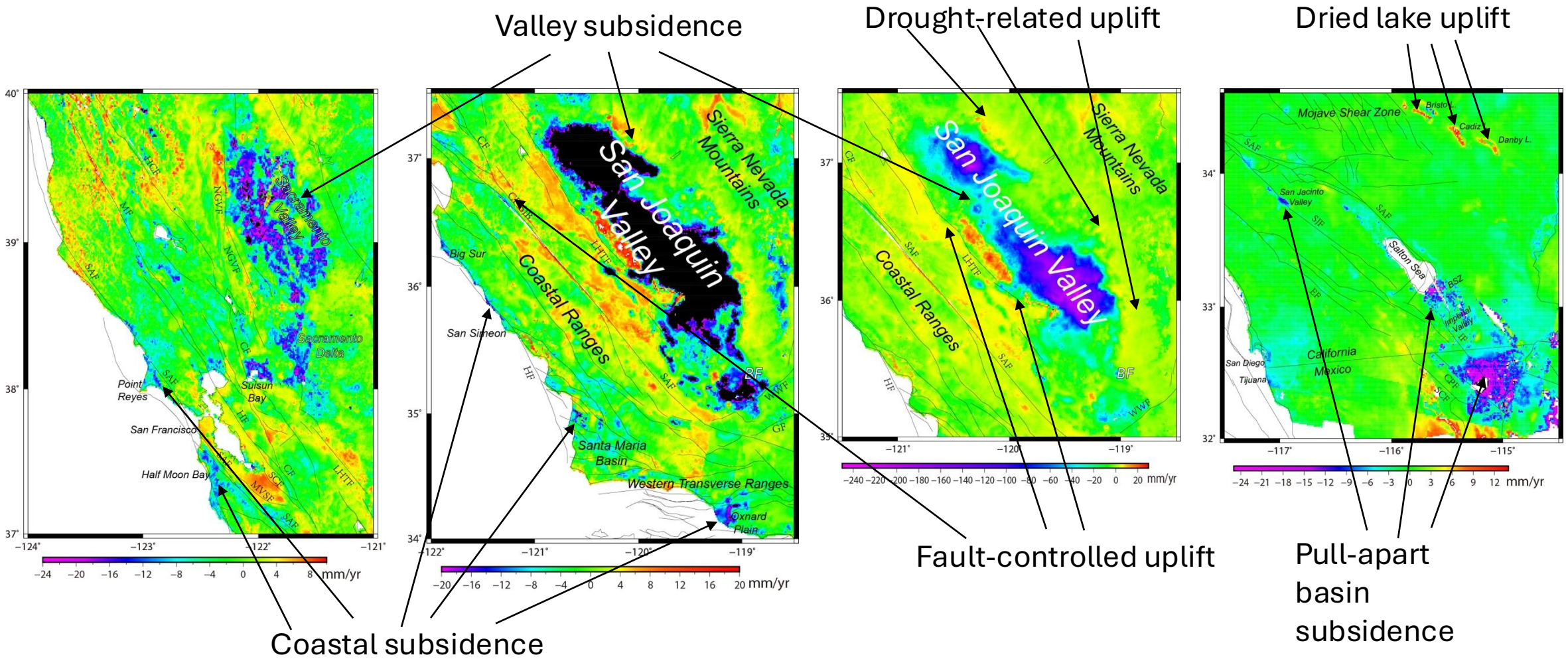

Fault Creep

Along strike component

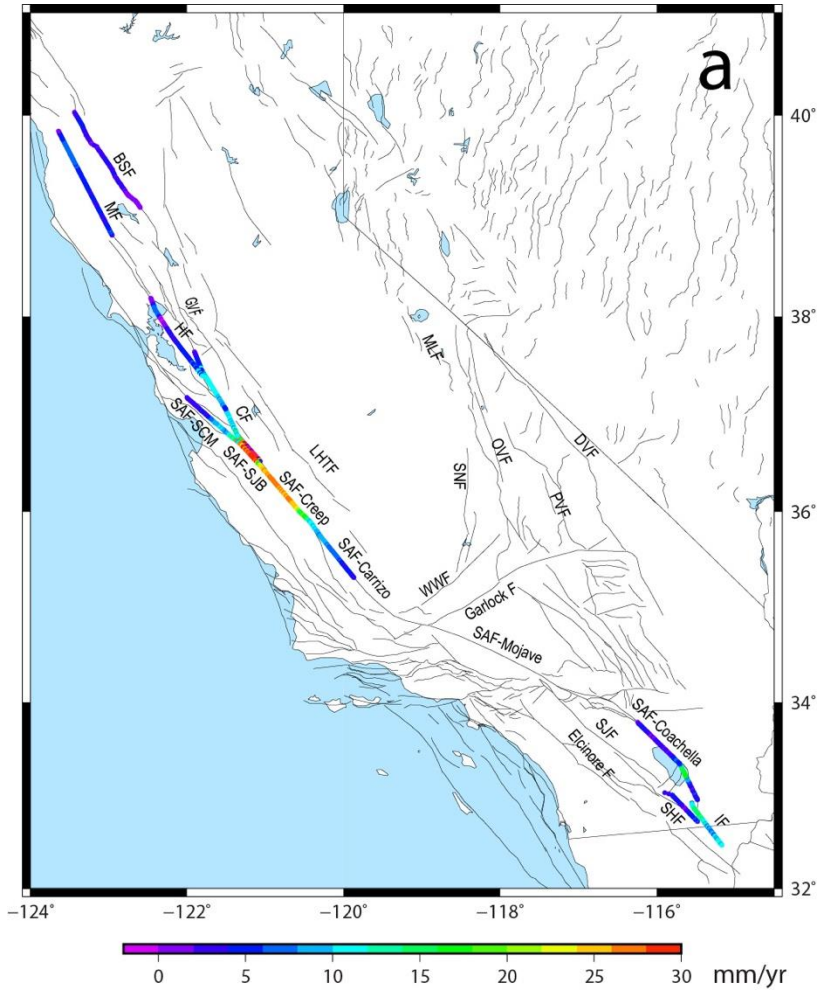

Vertical component

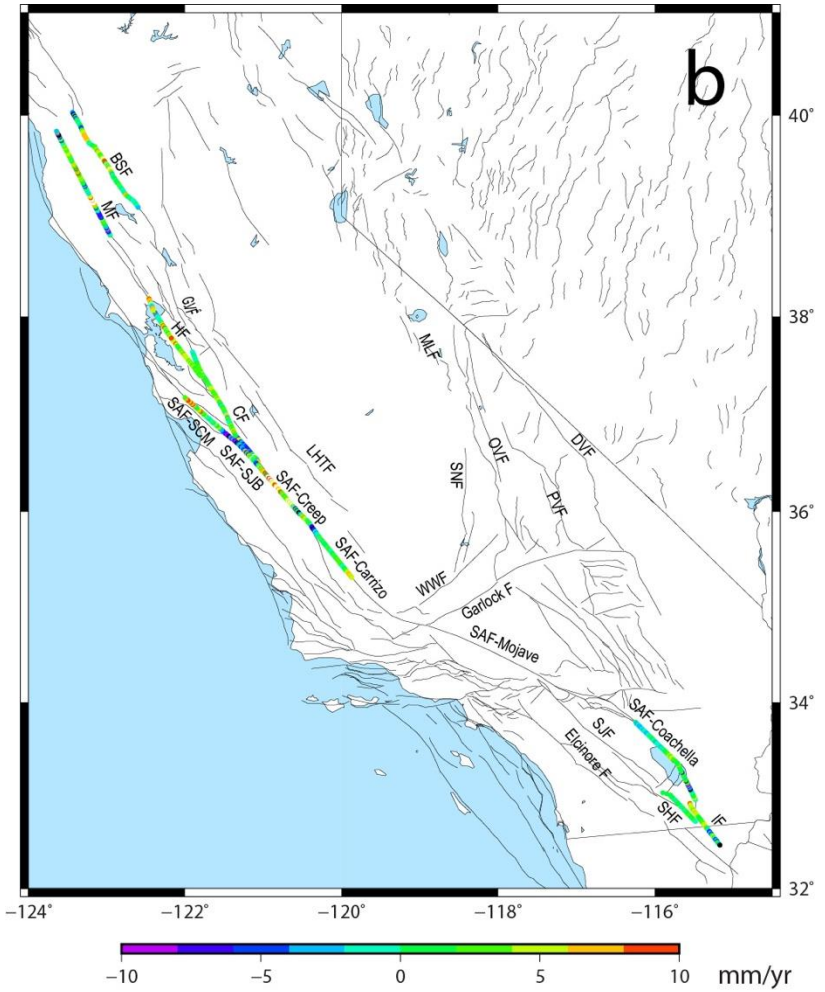

Comparison with Observations

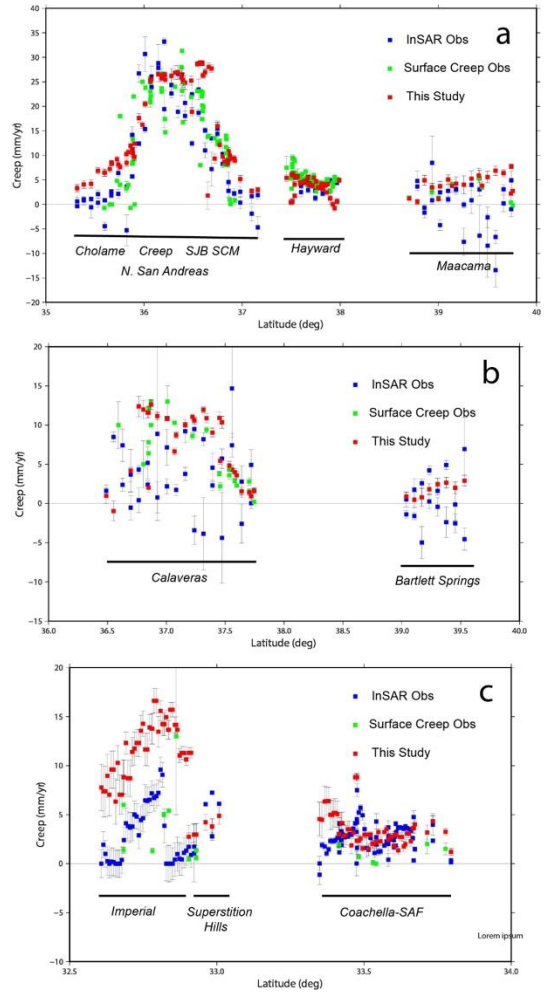

Significant surface creep is detected across the Coachella, Cholame, central creep, and San Juan Bautista sections of the SAF, and the Imperial, Superstition Hill, and Calaveras faults.

Strain rate components wrt relative plate motion direction

Shear strain parallel to PMD

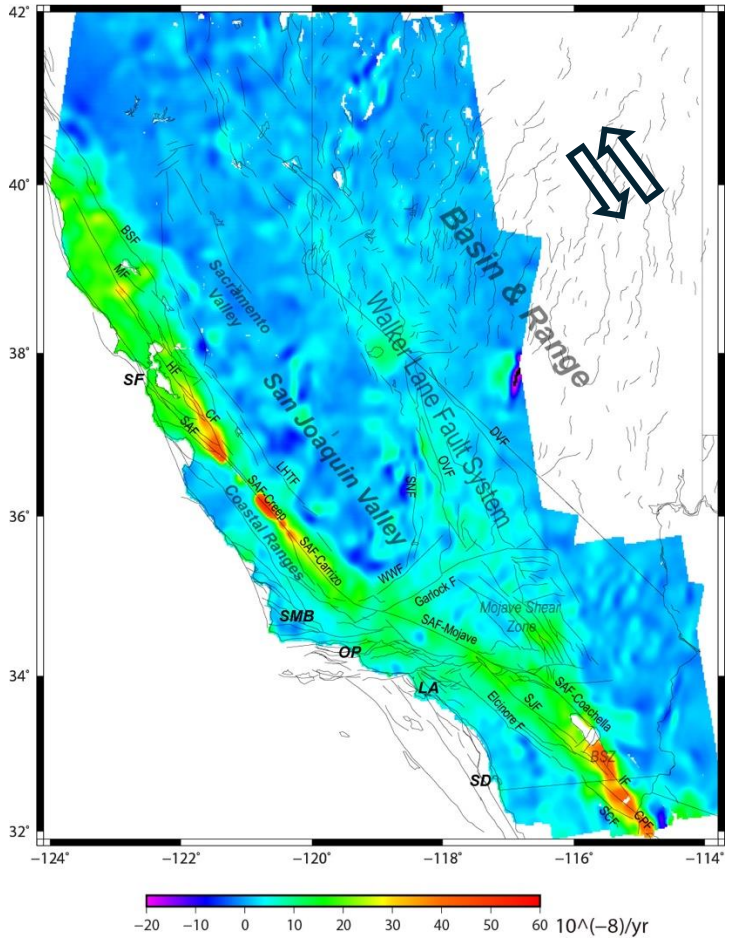

Normal strain parallel to PMD

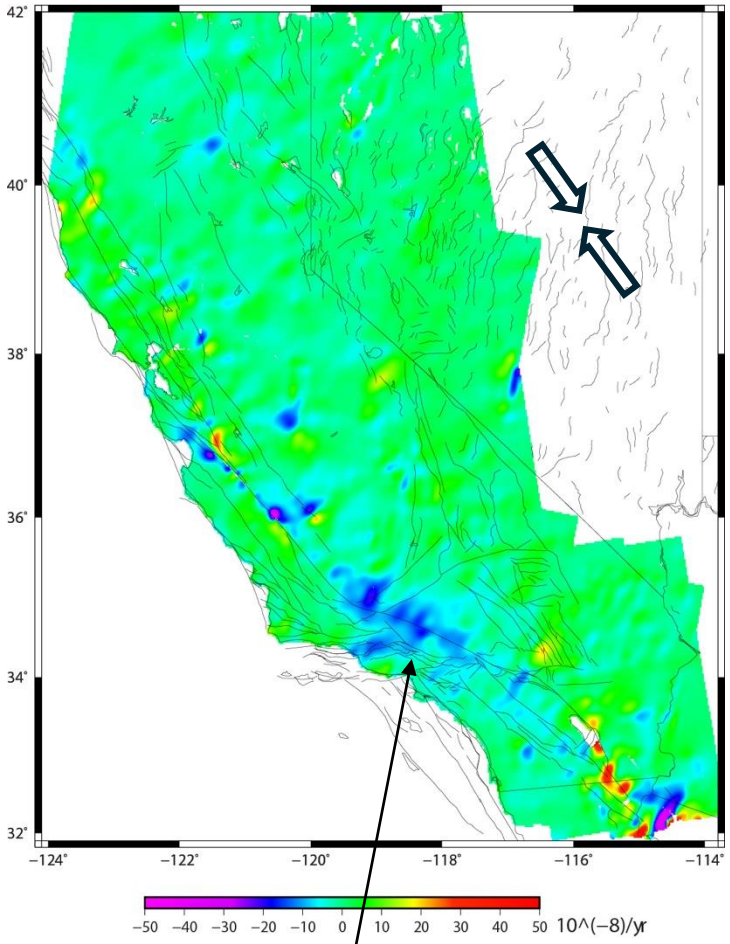

Normal strain perpendicular to PMD

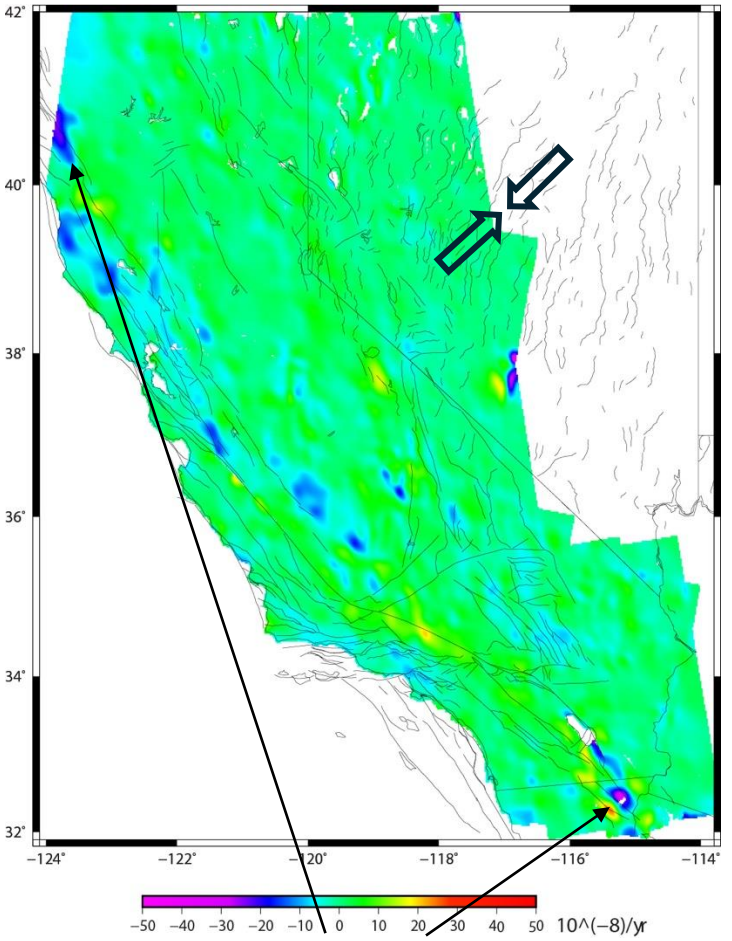

Significant deformation zones:

San Andreas & Walker Lane fault systems

SAF Big Bend & Western Transverse Ranges

Upper plate of Cascadia subduction & right-step fault zones

Comparison with fault-based deformation models

- Horizontal crustal deformation in California and western Nevada is dominated by tectonic deformation around the SAF and Walker Lane fault systems, and most of the deformation field can be interpreted as caused by slip underneath the known tectonic faults in the region, but the residual deformation field is also significant and broadly distributed.
- The mismatch between the observed and fault model interpreted deformation field is particularly significant across the Walker Lane fault system, possibly resulting in underestimation of accumulated seismic moment and earthquake potential in the region.

Reference

Hatem, A. E., Reitman, N. G., Briggs, R. W., Gold, R. D., Thompson Jobe, J. A., & Burgette, R. J. (2022). Western US geologic deformation model for use in the US National Seismic Hazard Model 2023. Seismological Society of America, 93(6), 3053-3067.

Shen, Z. K., & Bird, P. (2022). Neokinema deformation model for the 2023 update to the US National Seismic Hazard Model. Seismological Society of America, 93(6), 3037-3052.

Zeng, Y. (2022b). A Fault-Based Crustal Deformation Model with Deep Driven Dislocation Sources for the 2023 Update to the US National Seismic Hazard Model. Seismological Society of America, 93(6), 3170-3185.

Velocity Component Parallel to RPM

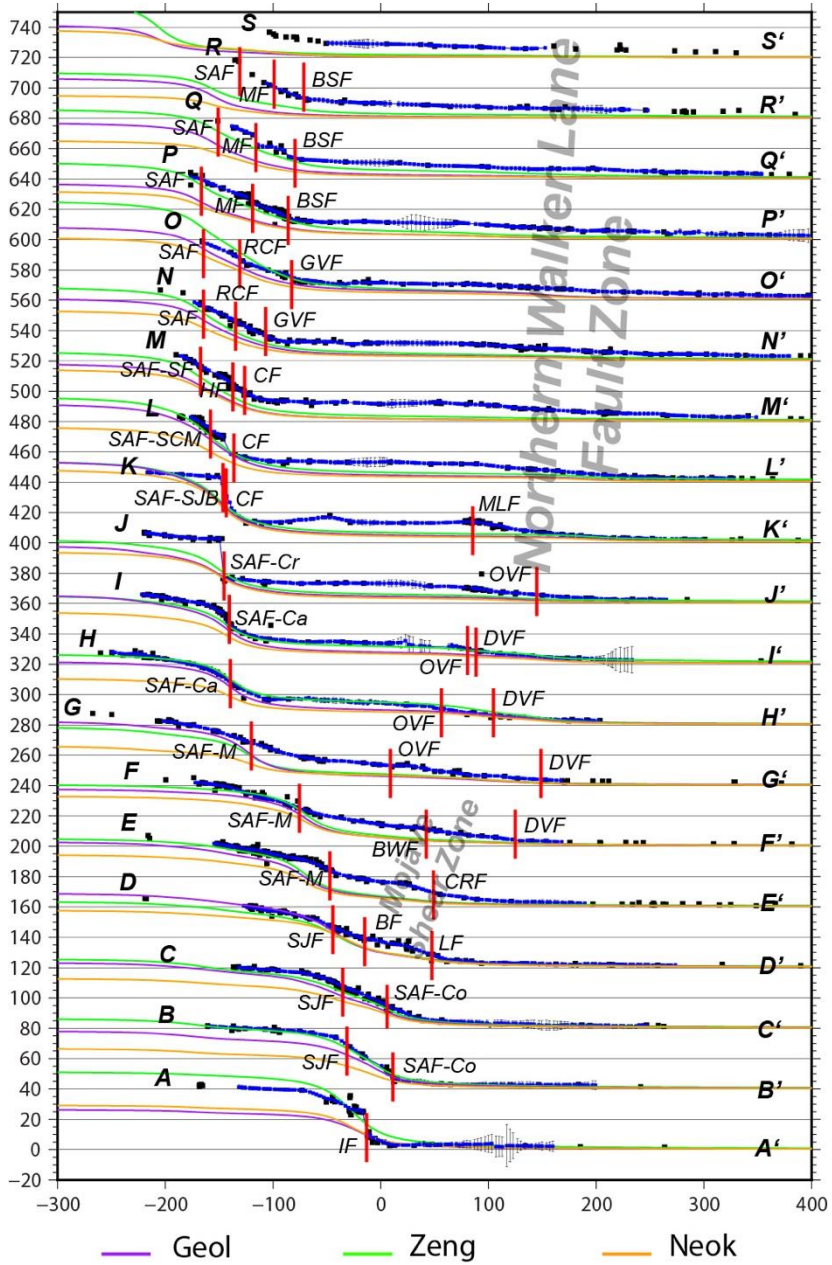

Issue to be addressed:

Temporal nonlinear deformation, particularly in regions severely affected by hydrologic activities

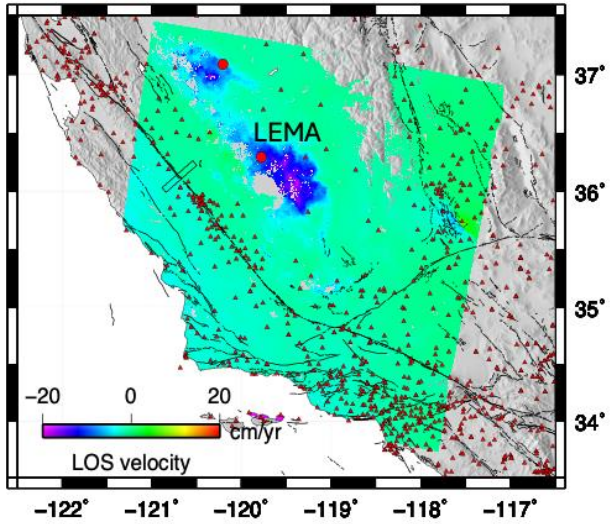

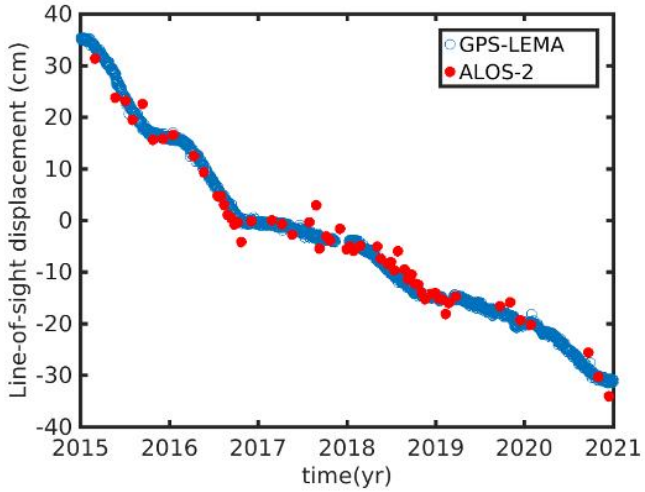

D144: 2014/11/08-2019/01/22

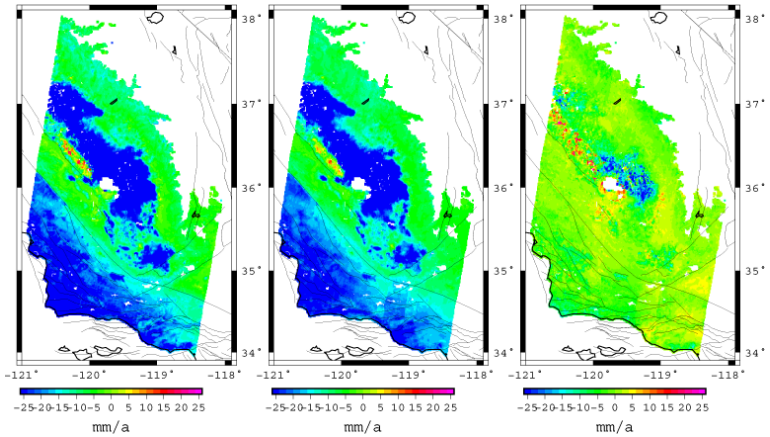

2015/03/01-2019/07/04D167:

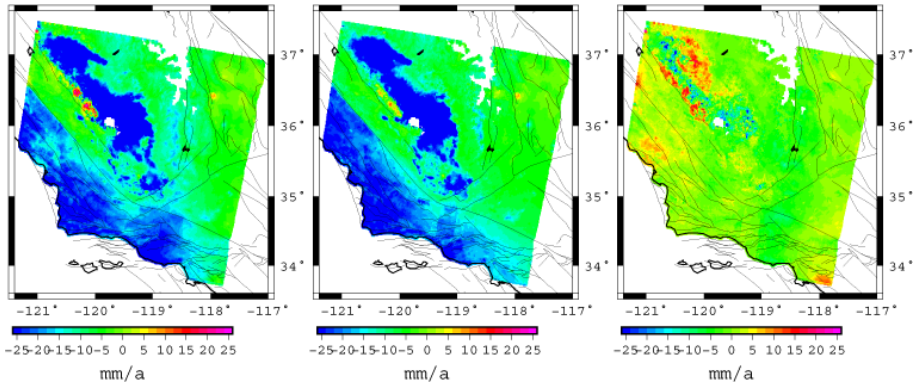

D168: 2015/02/20-2020/12/04

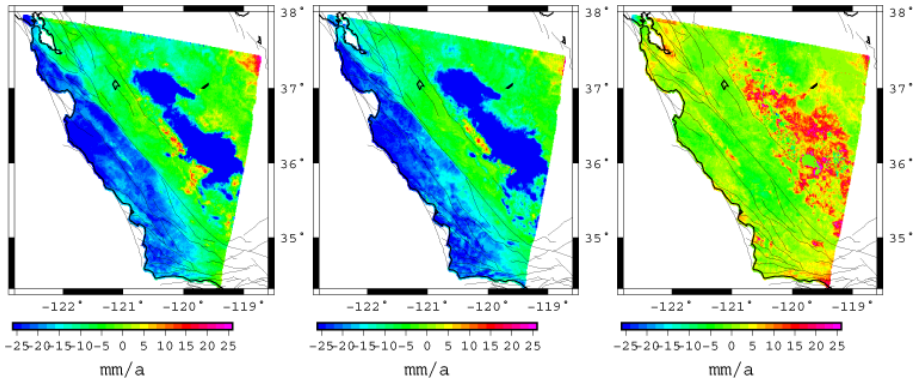

Issue to be addressed:

Short-wavelength variation of velocity field solution ($dV/dL \sim 10^{-9}$ radian/yr), resulting in instability of interpolated strain rate field

Maximum Shear Strain Rate

Smoothing Distance = 5 km

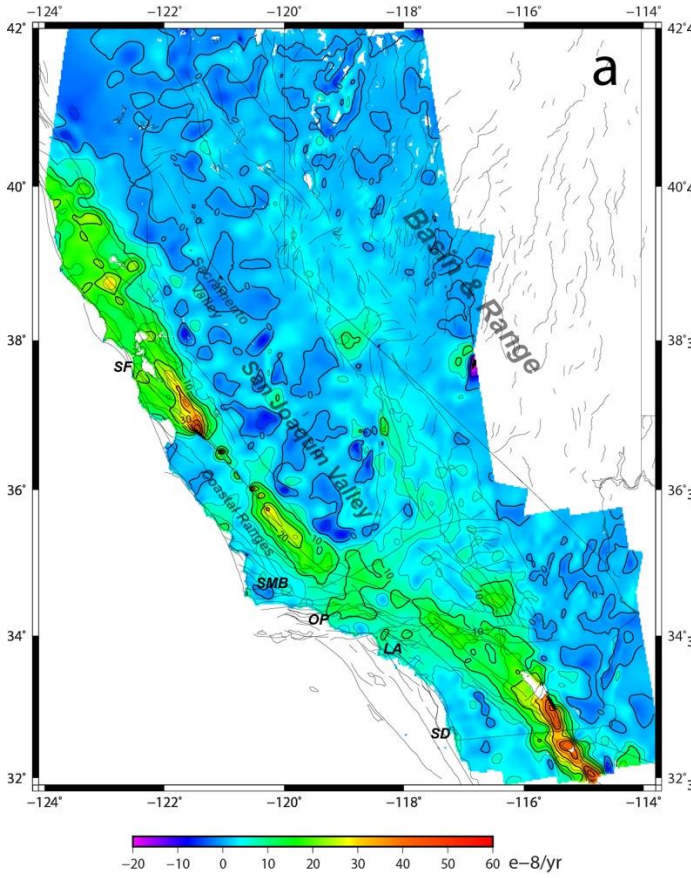

Smoothing Distance = 3 km

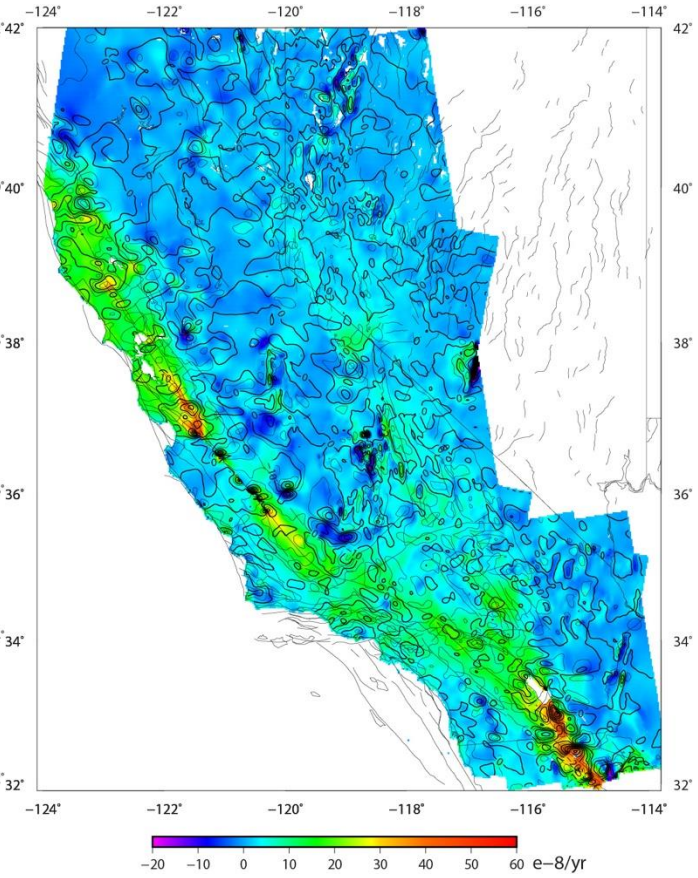

Summary

Developed a method to optimally integrate GNSS and InSAR data. The approach includes:

- Realistic assessment of GNSS data uncertainties
- Optimal interpolation of GNSS data
- Realistic rescaling of InSAR data uncertainties
- Optimal estimation of offset/ramp parameters and removal of the effect from InSAR data
- Integration of GNSS and InSAR to solve for 3-D deformation by least-squares regression, weighted by the adjusted GNSS and InSAR data uncertainties

Application of the method to California/western Nevada provides a solution of 3-D continuous deformation field, and helps resolve:

- Detailed deformation field across faults
- Fault creep
- Off-fault strains
- Pattern of tectonic deformation related to distribution of seismic moment
- Hydrologically related deformation mainly in vertical component, at various locations such as subsidence in valleys, along coastal lines, and at pull-apart basins, gradient across faults, and uplift at dried lakes, etc.

Thank you!

GNSS and InSAR Data Integration Procedure

- Develop an optimal approach to interpolate discrete GNSS velocity data points into a continuous velocity field [Shen and Liu, 2020]
- Adopt a realistic approach to evaluate uncertainties for InSAR and GNSS measurements and the interpolated GNSS velocities, to be used as weights in the combination
- Resolve the ramp parameters of multiple tracks of InSAR data through global optimization to minimize systematic biases in the solution
- Take an average of InSAR LOS data within small grids and integrate the deramped InSAR and interpolated GNSS data in the grids to solve for 3-D deformation through least-squares regression.

2nd invariant strain rate

Horizontal strain rates are ~0.2-0.6 micro-rad/yr across the SAF and ~0.05-0.15 micro-rad/yr across the Walker Lane fault systems

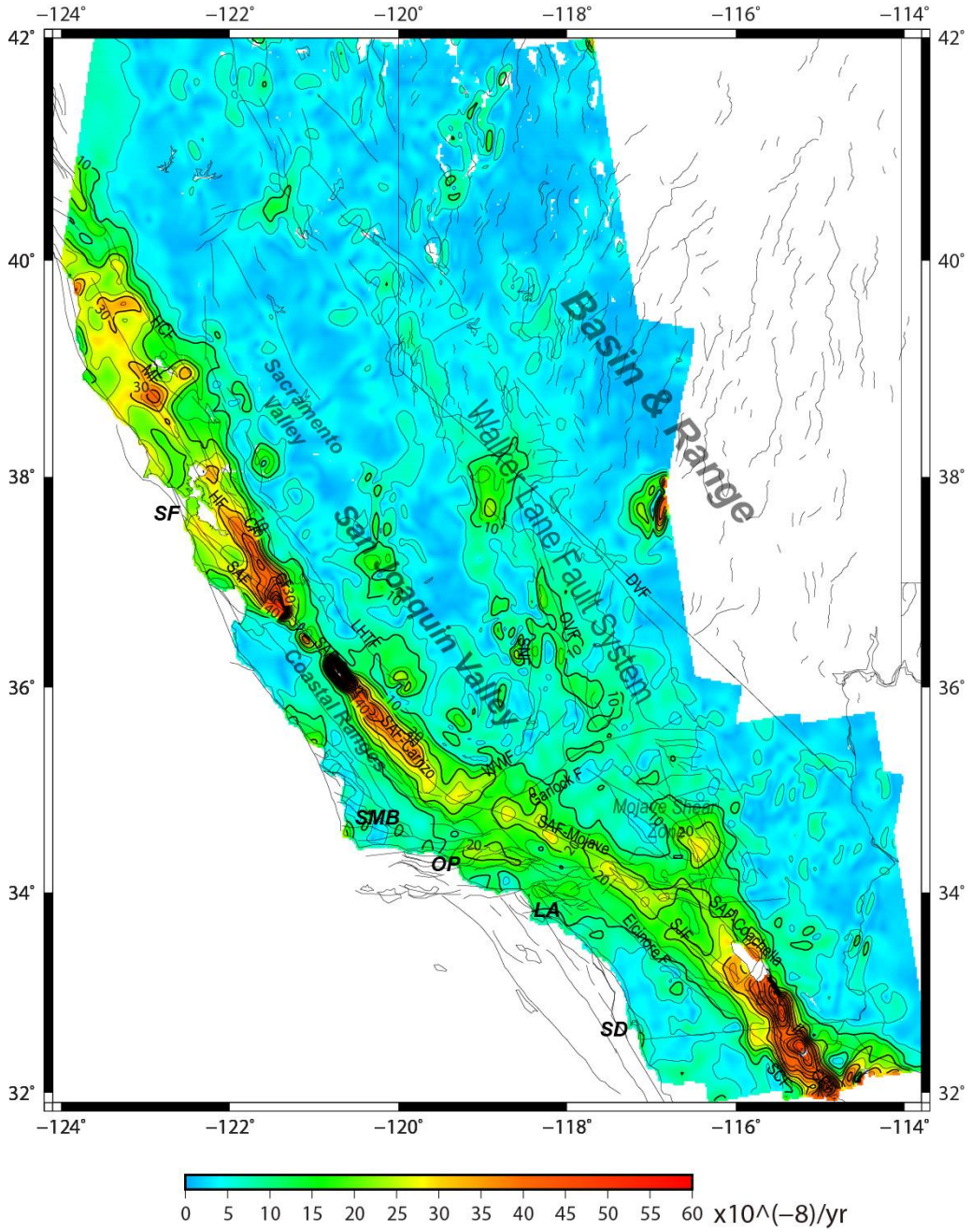

GNSS and InSAR (grid averaged LOS rate) data comparison

The InSAR data uncertainties are rescaled using RMS of LOS rate differences between GNSS and InSAR LOS rates

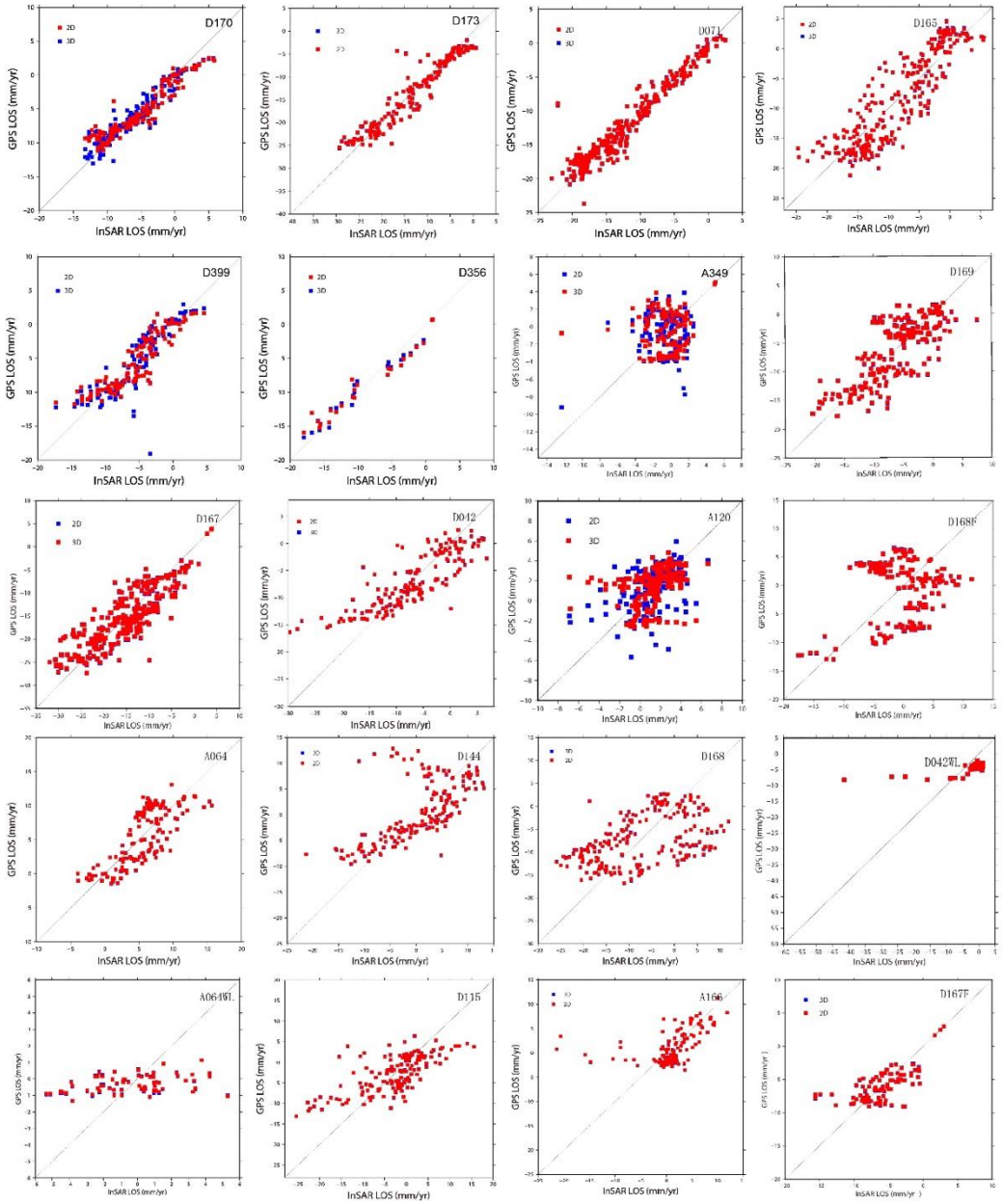

Integrated 3-D velocity field of California and western Nevada, with respect to stable North America. (a) and (b) are east and north velocity components, and (c) and (d) are their uncertainties, respectively.

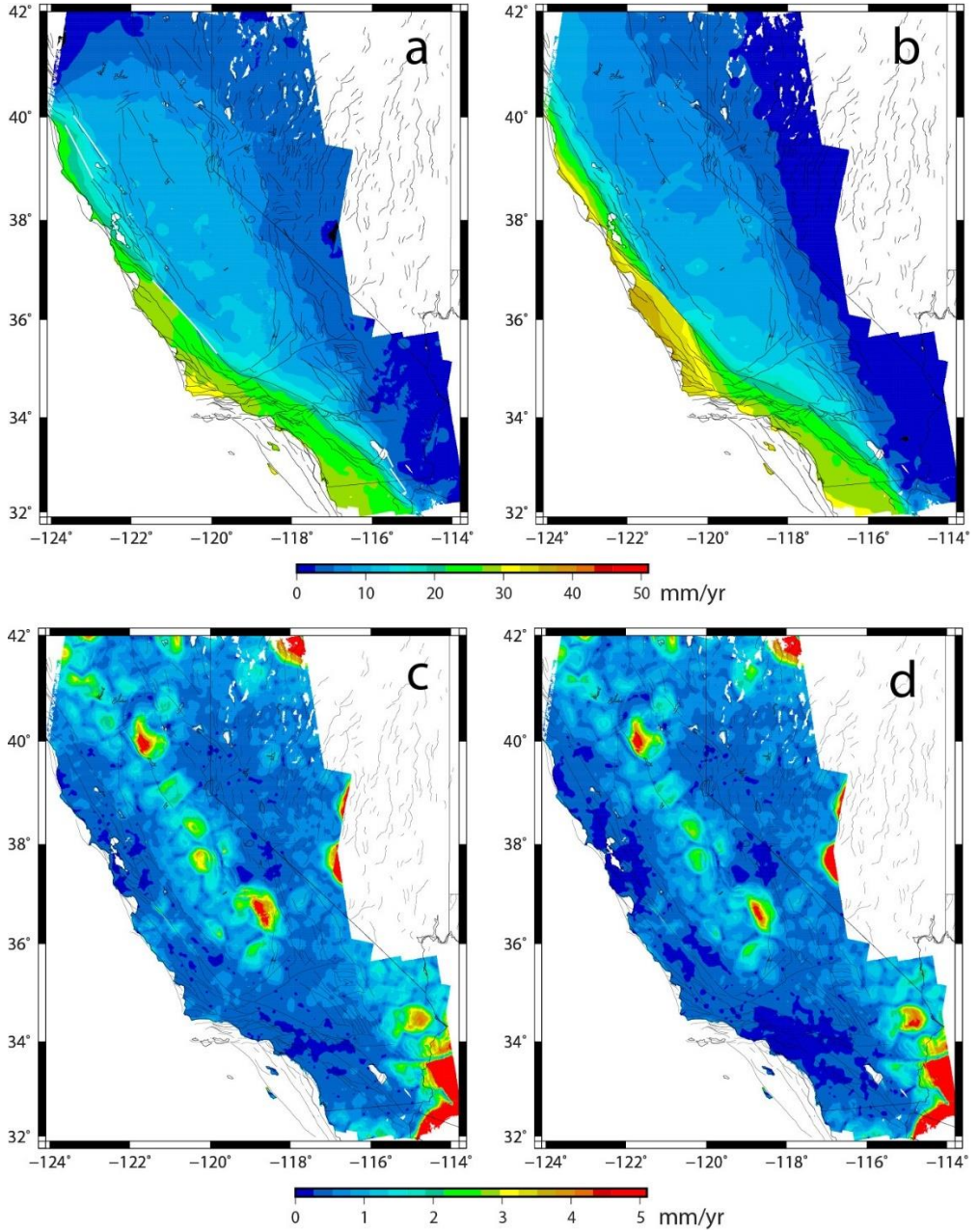

Uncertainty estimation for interpolated GNSS velocities

- **Cut-off velocity uncertainties for the horizontal and vertical components**: Using differential velocities of closely located station pairs to estimate the minimum (cut-off) velocity uncertainties: ~0.4 mm/yr for the horiz. and ~0.6 mm/yr for the vert.
- **GNSS velocity interpolation**: The GNSS velocities are used in an optimal interpolation procedure to deduce the continuous velocity field, with variation of degree of smoothing determined by balancing a trade-off between the spatial resolution and solution stability [Shen et al. 2015, 2020].
- **Uncertainty estimation of interpolated GNSS velocity field**: Using bootstrapping algorithm to estimate the interpolated GNSS velocity uncertainties in an iterative way. Each time an a priori smoothing distance *D* is assumed and used uniformly to evaluate the interpolation velocity uncertainties (σ_a) at all the GNSS sites. In each interpolation the estimation is also performed at each GNSS site without using data of the site, and a difference (δ_d) is calculated at the site between the estimated and original site velocities. Two median uncertainty estimates among all the sites (σ_{am} and δ_{dm}) are compared with, and another iteration is run with a new a priori smoothing distance *D*, until the two median uncertainties are about equal.